Numerical investigation of organic light emitting diode OLED with different hole transport materials

S. Mehdi, R. Amraoui, A. Aissat*
LATSI, Laboratory, Faculty of Technology University of Blida.1, 09000 Blida, Algeria

In this paper, a comparative study between four OLEDs devices is carried out. The bi-layers device (A) (consists of) Hole Injection Layer (HIL)/Electron Transport Layer (ETL), the multilayer device (B) (consists of) HIL Layer/Hole Transport Layer (HTL)/ETL Layer. The influence of the hole transporting material on the performance of the three layers OLEDs was investigated. Three different HTL materials were used: α-NPD, TAPC and p-TTA with the same electron transporting material as Alq_3; (these holes transport material consists the devices (B), (C) and (D) respectively). The carrier injection, Langevin recombination rate, singlet exciton density and the power of luminescent are demonstrated. The simulation results shows that the insertion of a thin HTL layer between HIL and ETL layers increases the characteristics of the device (B)as: $6.19.10^{25}$ $cm^{-3}s^{-1}$ of the Langevin recombination rate, $1.16.10^{15}cm^{-3}$ of the singlet exciton density and 0.04232 $W/\mu m^2$ of the luminescence power. Moreover, the insertion of TAPC as HTL material gives rise to $1.36.10^{26}$ $cm^{-3}s^{-1}$ of the Langevin recombination rate, $2.10^{15}cm^{-3}$ of the singlet exciton density and 0.075 $w/\mu m^2$ of the luminescence power.

(Received January 3, 2022 ; Accepted July 15, 2022)

Keywords: Turn on voltage, Single exciton density, Langevin recombination rate, Luminescence power

1. Introduction

Organic Light Emitting Diode (OLED) [1] based on small organic molecules and polymers PLED (Polymer Light Emitting Diode) have been widely studied during these past two decades. This is due to their promising applications in flat panel display like computer monitors, smartphone, tablet, notebooks and TV panels …etc, and will be widely used in solid state lighting such as residential, outdoor, commercial building, auto motivate, etc [2]. There are two types of OLEDs, according to the mode of operation: AMOLED with active matrix or PMOLED with passive matrix constitute the pixels of thin flexible TV display [3-4]. The OLEDs present an excellent performance in size (ultra thin displays), high brightness, high contrast, flexibility and wide viewing angle with a weak application voltage and switching time fast enough [5-6]. The first organic electroluminescence OLED was demonstrated in 1987 by Tang and VanSlyke [1, 7], this device consisted of HTL and ETL which serve as an Emissive Layer (EML). To acquire an effective OLED there is a weak injection barrier for holes between the Highest Occupied Molecular Orbital (HOMO) levels of the organic layers (HTL/EML). The electrons confinement in the EML layers reached with the high energy barrier for electrons between the Lowest Unoccupied Molecular Orbital (LUMO) levels of the organic layers (HTL/EML). Consequently, the recombination zone will be in EML [8-11]. To enhance the efficiency of OLED, the multilayer structures have been developed [7, 12-22].

We have used 4,4',4''-Tris {N-(1-naphthyl1)-N-phenylamino}-triphenylamine (1-naphdata) as the HIL layer, and N, N' – di (naphthalene-l-yl)- N,N' – dipheny libenzinide (α-NPD) as the HTL layer ,and 8-hydroxyquinoline aluminum (Alq_3) as ETL layer. For the devices (C) and (D) we have used 1,1-bis[4-[N,N-di(p-tolyl) amino]phenyl]cyclohexane (TAPC),tri(p-terphenyl-4-yl)amine (p-TTA) respectively as HTL materials [10], these materials exhibited higher mobility

* Corresponding author: sakre23@yahoo.fr
https://doi.org/10.15251/DJNB.2022.173.781

then that α-NPD ($6.14.10^{-4}$ $cm^2v^{-1}s^{-1}$): $\mu_h = 1.10^{-2}$ $cm^2v^{-1}s^{-1}$, $\mu_h = 6.9.10^{-3}$ $cm^2v^{-1}s^{-1}$, respectively [23, 24].

Our work aims to demonstrate that multi-layered OLEDs (Organic Light Emitting Diode) are more efficient than the two-layered OLEDs. On one hand, it has been proving that the injection of carriers in equilibrium (reduces non-radiative recombinations) and the position of the recombination zone is close to the center of the component, are two basic conditions for having better luminescence power. On the other hand, it has been shown that TAPC is a better material to use as the hole transporter due to: high mobility and high LUMO 2.0eV level, which prevents the movement of electrons towards the anode. Thus reducing the leakage current and keeping them confined to the TAPC / EML interface. The carriers injection density, Langevin recombination rate, singlet exciton density and the power of luminescent are demonstrated.

2. Theoretical model

The electrical transported inside the OLED can be modeled by the one-dimensional time independent drift-diffusion model [28-30]:

$$\frac{\partial E(x)}{\partial x} = \frac{q}{\varepsilon\varepsilon_0}(p(x) - n(x)) \tag{1}$$

The electric field in the device is calculated by the following equation:

$$V_{applied} - V_{bi} = \int_0^L E(x)dx \tag{2}$$

where:

$V_{applied}$ is the applied voltage across the device.

V_{bi} built in- potential due to the difference in work functions of electrode material.

L is the total layer thickness, in our case 100nm.

Charge carriers transport through drift (electric field driven) and diffusion (density gradient driven) [28] are:

$$j_n(x) = e.\left(\mu_n.E(x).n + D_n.\frac{\partial n}{\partial x}\right) \tag{3}$$

$$j_{p(x)} = e.\left(\mu_p.E(x).p + D_p.\frac{\partial p}{\partial x}\right) \tag{4}$$

The mobility of organic material is calculated by the Pool-Frenkel equation [28, 30] as follow:

$$\mu_n(E) = \mu_{n0}(E).\exp\left(\gamma_n.\sqrt{E}\right) \tag{5}$$

$$\mu_p(E) = \mu_{p0}(E).\exp\left(\gamma_p.\sqrt{E}\right) \tag{6}$$

where:

μ_{n0} , μ_{p0} are respectively electrons and hole mobility at zero electric field.

γ_n, γ_p are the Pool-Frenkel factor describing field dependence.

The recombination of holes and electrons to exctions occurs due to attractive Coulombic interaction. The bulk recombination rate of free holes and electrons is calculated in accordance with Langevin theory [30].

$$R = \frac{e}{\varepsilon.\varepsilon_0}.\left(\mu_n + \mu_p\right) \tag{7}$$

where:

R is the recombination rate.

$\mu_n(\mu_p)$ is the electron (hole) mobility
$n(p)$ is the electron (hole) density

The continuity equations [29] are:

$$\frac{\partial n}{\partial t} = \frac{1}{e}\frac{\partial j_n}{\partial x} - R - \frac{\partial n_t}{\partial t} \quad (8)$$

$$\frac{\partial p}{\partial t} = \frac{1}{e}\frac{\partial j_p}{\partial x} - R - \frac{\partial p_t}{\partial t} \quad (9)$$

n_t , p_t are trapped carries.

The trapped electrons and holes equations are [29]:

$$\frac{\partial n_t}{\partial t} = r_c n(N_t - n_t) - r_e . n_t \quad (10)$$

$$\frac{\partial p_t}{\partial t} = r_c p(N_t - p_t) - r_e . p_t \quad (11)$$

where:
N_t is the trap density.
r_c is the capture rate, and r_e the emission rate.

The recombination of holes and electrons at the organic interface results in the formation of singlet and triplet exciton in a ratio of 1:3 due to spin statistics, fluorescence light emission due to radiative decay can only be expected from singlet exciton [1, 22-31].

The continuity equation of the singlet exciton is given by [29, 32]:

$$\frac{\partial S_i(x,t)}{\partial t} = G_i R(x,t) + \overrightarrow{\nabla J_{S1}}(x,t) - (K_{radi}(x,t) + K_{nonradi})S_i(x,t) - K_{annihilationi}S_i(x,t)^2 + \sum_{j=1}^{nexe}(K_{ji} . S_j(x,t) - K_{ij} . S_i(x,t)) \quad (12)$$

where:
G_i is the constant for generation efficiency.
K_{rad} is the radiative decay rate.
$K_{non\ radi}$ is the non-radiative decay rate.
$K_{annihila}$ is the annihilation rate.
$R$is the recombination bimolecular rate.
S_i is the singlet exciton.

3. Results and discussion

The structure and schematic diagram of energy levels of OLED based Alq3 as the electrons transport layer and emitting layer with three different holes transporting materials are presented in the figure.1. The four devices OLEDs, HIL/HTL/ETL structures as follows:

Device A: no HTL /1-naphdata (50nm)/Alq3 (50nm).
Device B: 1-naphdata (40nm)/ α-NPD (10nm)/ Alq3 (50nm).
Device C: 1-naphdata (40nm)/ TAPC(10nm)/ Alq3 (50nm).
Device D: 1-naphdata(40nm)/ p-TTA(10nm)/ Alq3 (50nm).

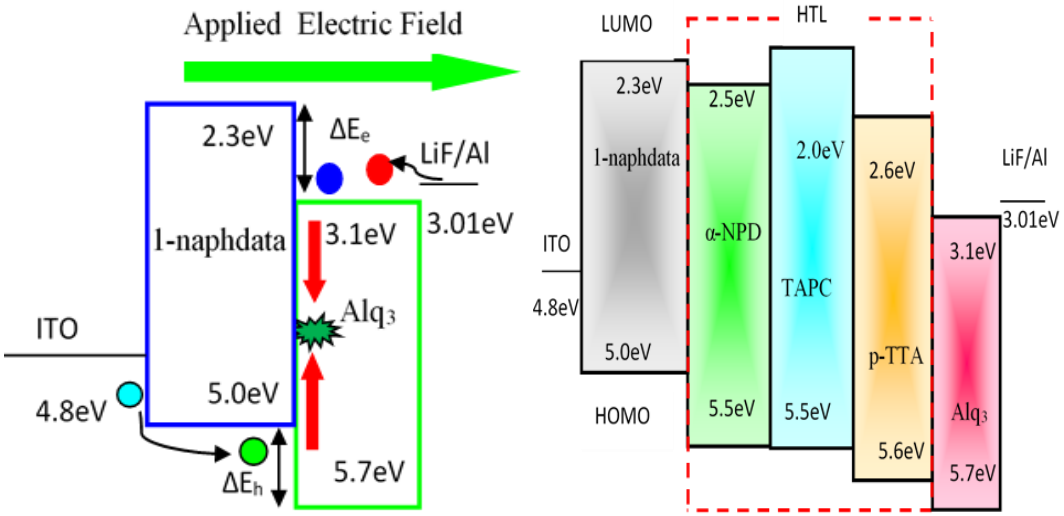

(a) *(b)*

Fig. 1. (a,b) . Schematic diagrams of energy levels of green fluorescent OLED based on $Alq_3$with three different HTL (α-NPD, TAPC, p-TTA) , (a) ITO/1-naphdata (50nm)/Alq_3(50nm)/LiF/Al, b) ITO/1-naphdata (40nm) /HTL(10nm)/Alq_3(50nm) /LiF/Al.

Table 1 shows various performances (Tg, mobility, HOMO and LUMO values) of reported hole transporting materials. By applying an electric potential difference of 7V between anode and cathode, the holes are injected from the anode toward the HOMO level of the HIL layer. At the same time, the electrons are injected from the cathode toward the LUMO level of the ETL layer. The injected charges migrate in the organic material toward the oppositely charged electrode under the influence of the electrical field and the recombination occurs at the heterojunction.

Table 1. Comparative values of energy level, Tg and electron mobility of electron transporting materials

Electron transporting materials [References]	Bphen [5,13]	Alq_3 [13,20-21]	TPBi [5,13]	TAZ [4,14]
HOMO (eV)	6.2	5.7	6.7	6.3
LUMO (eV)	2.9	3.0	2.7	2.7
T_g (C^0)	66	175	127	-
μ_e ($cm^2v^{-1}s^{-1}$)	$3.25.10^{-4}$	$1.51.10^{-7}$	$6.53.10^{-5}$	$1.57.10^{-6}$
μ_e ($cm^2v^{-1}s^{-1}$)		$8.05.10^{-6}$		

Comparative table including structure and results of some published references

Figure 2 represents the current voltage characteristics for fluorescent OLED based on different HTLs materials. The bi-layers device (A) has the lowest turn-on voltage 2.5V, whereas the α-NPB device (B), TAPC device (C) and p-TTA device (D) characteristics have an identical turn-on voltage which is 3.5V [10]. When the current set to 40mA, the operating voltage of the green fluorescent OLEDs based bi-layers device (A) was 4.3V and the three other devices have the same operating voltage of about 5V.

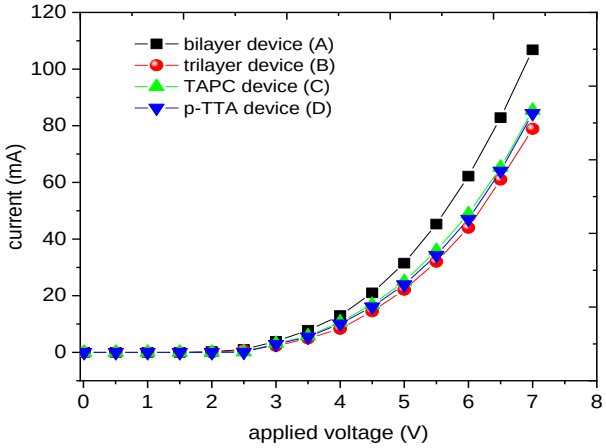

Fig. 2. I-V Characteristics of green fluorescent OLEDs for series of devices OLEDs (A-D) at 7V

Figure 3 (A, B, C, D) represents the distribution of the charge carriers density versus x position from the anode. The holes are accumulated at the front of the interface HIL/ETL (50nm) due to the difference between the HUMO levels ΔE_h.

The HIL layer transports the hole only and block the movement of the electrons injected from the cathode [18, 30]. While the electrons are accumulated at the front of the interface HIL/ETL due to the difference between the LUMO levels ΔE_e [3, 18, 30].

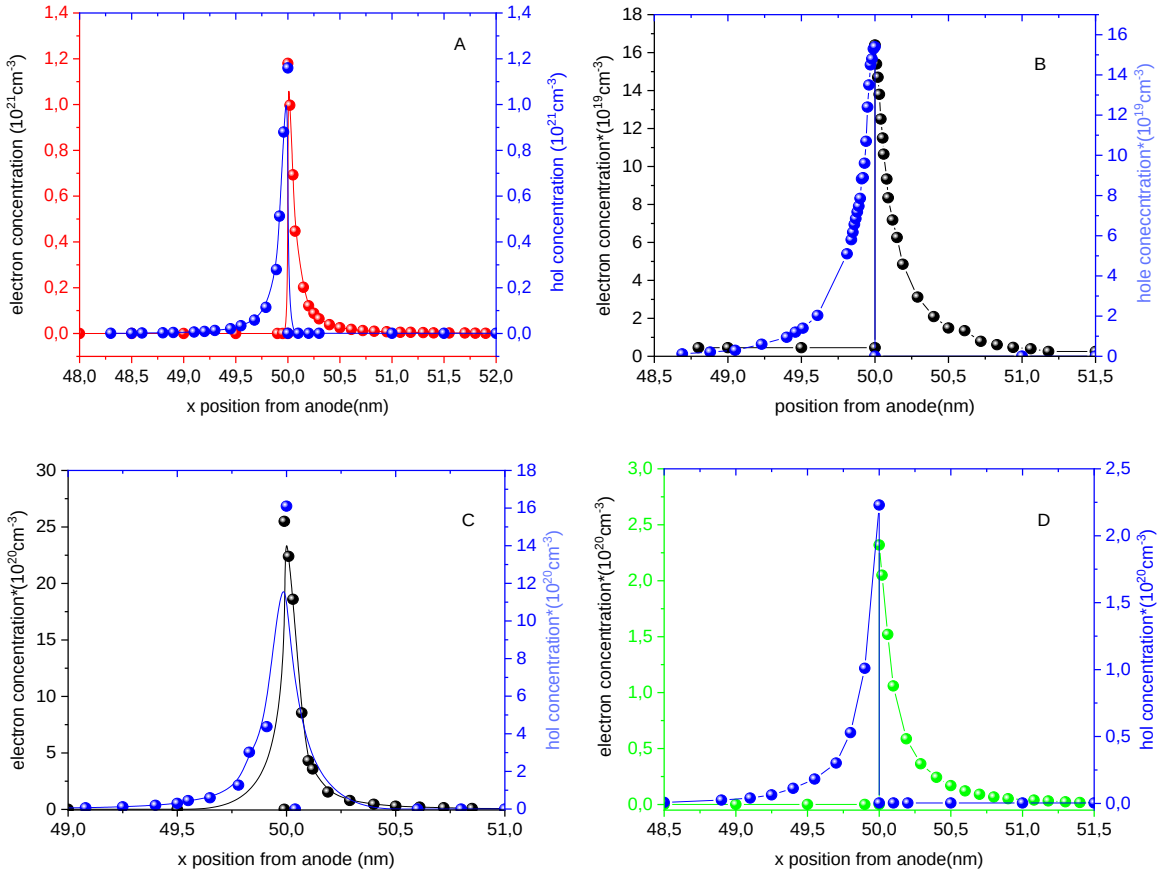

Fig. 3. Distribution of the charge carrier density in: device A (Fig. 3. A), device B (Fig. 3. B), device (Fig. 3. C), device D (Fig. 3. D).

We have balanced the charges concentration to $1.2.10^{21}cm^{-3}$ at the interface. The accumulated charges create the recombination zone [33, 34-38].

For the multilayer device (B), an intermediate layer has been added between the two layers HIL/ETL; the energetic HOMO and LUMO levels form an energetic barrier cascading "energetic-staircase" [18]. The holes will be crossing the barrier according to the difference between the HOMO levels from the two organic layers ΔE_h [12, 16].

The simulation results given in figures 3 (A, B, C, D) show that the charge carriers are accumulated at the interface HTL/ETL [36-39], with a reduction in interfacial charges density [2, 7, 10-12]. It was found that the device(C) with TAPC as HTL material has maximum charge carriers concentration due to its high hole mobility 10^{-2} $cm^2v^{-1}s^{-1}$ [10,23, 26], and we remark that the amount of the electrons concentration at the interface depends on the HTL material [10].

The Langevin recombination rate for a series of devices OLEDs (A-D) at 7V is given in figure 4. It was found that the radiative recombination of the free carriers injected (electrons and holes) take places in Alq_3 layer [10] and is located at about 20 Å from the interface HTL/ETL [10], which simultaneously serves the Emissive Layer (EML).

These results are in good agreement with Tang's finding [1, 14]); then the flux of photon will be reflected by the cathode. The free charge carriers recombination for the device (A) are confined to a very narrow region in EML with value $1.49.10^{25}$ $cm^{-3}s^{-1}$[10], and we have low recombination rate for the device (B) and (D) with α-NPD, p-TTA as HTL material respectively, due to the low holes mobility $6.1.10^{-4}$ $cm^2v^{-1}s^{-1}$ and $6.9.10^{-3}$ $cm^2v^{-1}s^{-1}$ respectively.

In addition, a large recombination zone was obtained with a value of $1.36.10^{26}$ $cm^{-3}s^{-1}$ in case of the device (C). This is due to a maximum free charge carriers concentration at the interface HTL/ETL, because TAPC has the highest holes mobility of about 10^{-2} $cm^2v^{-1}s^{-1}$ [26] and has an excellent LUMO value (2eV), was effective electrons blocking at the TAPC/ EML interface (ΔEe = 1.1eV) which is beneficial to the recombination of exciton in EML [26,30]).

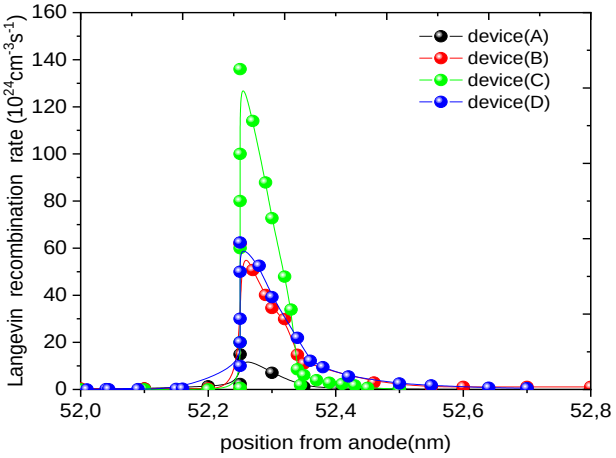

Fig. 4. Langevin recombination rate for series of devices OLEDs (A-D) at 7V.

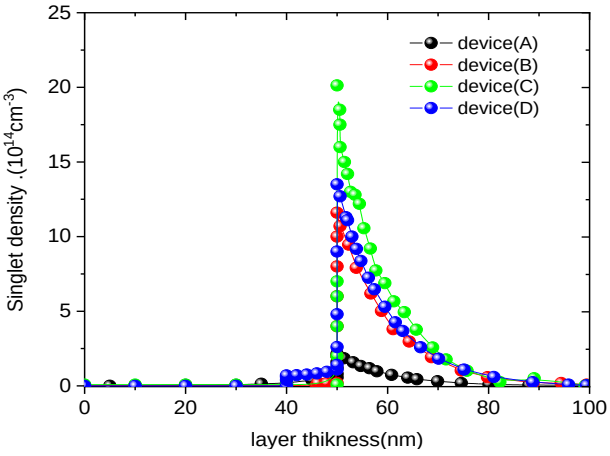

Fig. 5. Singlet density excitons for series devices OLEDs (A-D) at 7V.

On the other hand, we have observed the same results for the singlet exciton density represented in figure 5, because the Langevin recombination results in the formation of singlet and triplet exciton, with a ratio of 1:3 due to spin statistic; fluorescent light emission because of radiative decay can only be expected from singlet exciton [22, 31].

The exciton diffuses from the high to low concentration, and will be extended 30nm from the interface HTL/ETL and forming the emitting zone [40, 41]. The energy of the exciton emits a photon, the color of the light emitted may be chosen [6, 12]:

$$\Delta E = \frac{hc}{\lambda} \tag{13}$$

where:
λ is the emission wavelength.
h is the Planck constant ($6.626.10^{-34}$ J.S)

The validation of our numerical model is provided in figure 6. It shows the (J-L) characteristics for a series of OLEDs devices (A-D) with the experiment results of the reference [10], the agreement between our simulated results and measurements reference is acceptable. The luminance was calculated in (cd/m^2) by the relation [18,42]:

$$L = \eta_{\text{coup}}.K_m.S\,.h\nu.\frac{1}{\pi} \tag{14}$$

where:
K_m is the human eye sensitive K_m=683lm/W
S is the integrated exciton density.
hν is the energy of emitted photon

$$\eta_{coup} = \frac{1}{2n^2} \tag{15}$$

where:
n is the refractive index of the organic material (n=1.6).

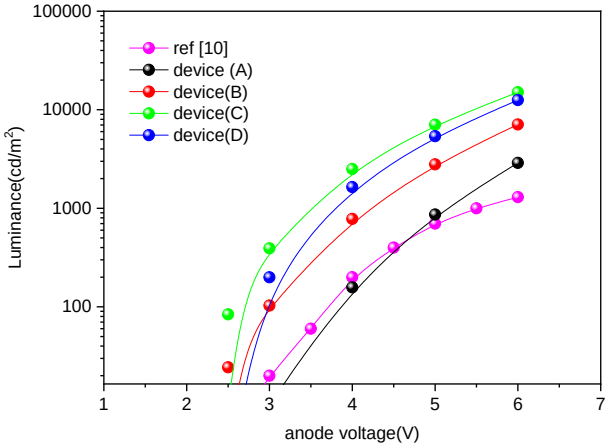

Fig. 6. L-V characteristics for series of devices OLEDs (A-D) at 6V compared with reference [10].

Table 2 summarize the structures to study compared with that of the references [28,33]. The luminescence power spectra versus voltage for a series of OLEDs devices (A-D) are represented in the figure 7, these results are in good agreement to be compared with previously stated data.

Table 2. Comparative table including differences structures and reference [28,33].

	Turn on voltage (V)	Langevin recombination rate ($cm^{-3}s^{-1}$)	Power of luminescence (w/µm)	References
Device A	2.5	$1.49.10^{25}$ 2.10^{20}	$9.93.10^{-3}$	[33]
Device B	3.5	$6.19.10^{25}$ 3.10^{24}	0.043	[28]
Device C	3.5	$1.36.10^{26}$	0.075	
Device D	3.5	$6.24.10^{25}$	0.05	

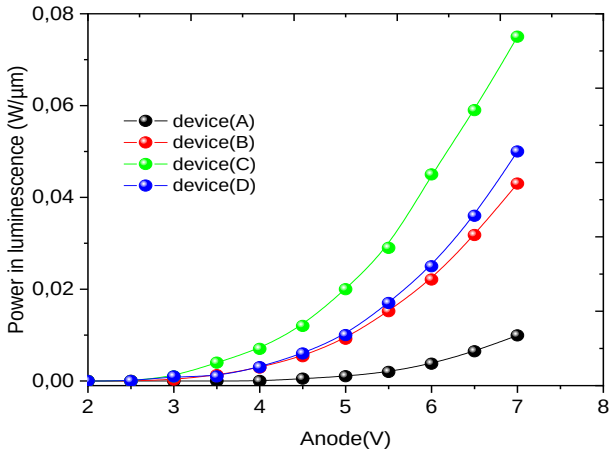

Fig. 7. Power of luminescence for series of devices OLEDs (A-D) at 7V.

The device (A) has the minimum luminescence power ($9.93.10^{-3}$ w/µm^2) the low efficiency can be explained by the inefficient generation of the bulk exciton in EML since the barrier height for charge carriers interface HIL/ETL crossing are relatively high [33]. For device (B), the insertion of the holes transport layer (HTL) decreases the direct interface recombination since the energetic barrier for the holes is reduced, the recombination interface becomes a very effective source for the bulk exciton [7, 12, 18]. We have an enhancement in the luminescence power of 0.043 W/µm^2 [2, 12]. For the device(D) with p-TTA as HTL material, we have slight difference in the luminescence power 0.05 W/µm^2 due to its high holes mobility ($6.9.10^{-3}$ cm^{2}v^{-1}s^{-1}) as compare to the mobility of that widely used α-NPD (6.10^{-4} cm^{2}v^{-1}s^{-1}) as HTL material [10]. For the device (C) the electrons blocking barrier at the EML layer lead to a maximum luminescence power 0.075 W/µm^2. Such performances are mainly attributed to good hole mobility and to the high LUMO level (2eV) for electrons blocking. We can say that the luminescence power is strongly related to the number of exciton generated in EML and the balance between the electron and hole in EML [26, 43].

4. Conclusion

The present work of simulation consists to study a series of devices OLEDs (A-D), for the two layers device a low luminescence power is obtained $9.93.10^{-3}$ w/µm^2. For the three layers device with α-NPD as HTL material, we have shown a large luminescence power 0.043 w/µm^2, this is due to a high density singlet exciton $1.16.10^{15}$cm^{-3}. Then, we used TAPC, p-TTA as hole transport layer and Alq_3 electrons transport layer and emissive layer, the device consists of holes transporting material as TAPC showed better characteristics, due to its high holes mobility (1.10^{-2}cm^{2}v^{-1}s^{-1}) and to the excellent LUMO level 2.0eV. We have obtained a maximum luminescence power of 0.075w/µm^{2}and an important singlet exciton density of 2.10^{15}cm^{-3}. We conclude that the performances of the OLED are controlled by the type of HTL materials used (T_g, mobility) also by the energetic barrier of HTL/ETL interface. We believe that TAPC can be a promising HTL material for the future applications in OLEDs.

References

[1] C. W. Tang, S. A. Van Slyke, Appl. Phys. Lett. 51(12), 913(1987) ; https://doi.org/10.1063/1.98799

[2] M. Singh, J.H. Jou, S. Sahoo, Sujith S. S, Z.K.He, G.Krucaite, S.Grigalevicius, C.W. Wang, Scientific Reports 8(1), 7133(2018) ; https://doi.org/10.1038/s41598-018-24125-4

[3] C. Lin, T.T.,Tsai, Y.C.Chen, Journal of Display Technoloy 4(1),54(2008) ; https://doi.org/10.1109/JDT.2007.901555

[4] C. Qiu, H. Chen, M. Weng, H. S. Kwok, IEEE Transactions on Electron Devices 48(9), 2131(2000) ; https://doi.org/10.1109/16.944206

[5] S.J. Zou, Y. Shen, F.M. Xie, J.D. Chen,Y.Q. Li, J.X.Tang, Mater. Chem. Front. 4, (788)2020 ; https://doi.org/10.1039/C9QM00716D

[6] L. S. Hung, C.H. Chen, Materials Science and Engineering R 39(5-6), 143(2002) ; https://doi.org/10.1016/S0927-796X(02)00093-1

[7] S .Ho, S. Liu, Y. Chen, F.So, Journal of Photonics for Energy 5(1), 057611(2015) ; https://doi.org/10.1117/1.JPE.5.057611

[8] B. Geffroy, P. le Roy, C. Prat, Polym. Int. 55(6), 572(2006) ; https://doi.org/10.1002/pi.1974

[9] F. Kozłowski, "Numerical simulation and optimisation of organic light emitting diodes and photovoltaic cells", Thesis, University of Dresden , 2005.

[10] S. Sato, M.Takada, D. Kawate, M.Takada, T.Kobayashi, H.Naito, Japanese Journal of Applied Physics 58(SF), SFFA02(2019) ; https://doi.org/10.7567/1347-4065/ab0de7

[11] R.A.K. Yadav, D.K. Dubey, S.Z. Chen, S.S. Swayamprabha, T.W.Liang, J.H.Jou, MRS

Advances 3(59),3445(2018) ; https://doi.org/10.1557/adv.2018.365
[12] A. Uniyal, S. P. Mittal, International Conference on Computing, Communication and Automation (ICCCA), 1505(2016).
[13] W. Brutting, S. Berleb, A.G. Mückl, Organics Electronics 2(1), 1(2001) ; https://doi.org/10.1016/S1566-1199(01)00009-X
[14] J. Chan, A.D. Rakic, Y.T. Yeow, A.B. Djurisic, Conference on Optoelectronic and Microelectronic Materials and Devices IEEE. , 53(2005).
[15] C. Adachi, T. Tsutsui, S. Saito, Appl. Phys. Lett. 57(6), 531(1990) ; https://doi.org/10.1063/1.103638
[16] H. Wang, K. P. Klubek, C. W. Tang, Appl. Phys. Lett. 93(9), 093306(2008) ; https://doi.org/10.1063/1.2978349
[17] Y. Karzazi,, J. Mater. Environ, Sci. 5(1), 1(2014).
[18] J. Staudigel, M. Stößel, F. Steuber, J. Simmerer, J. Appl. Phys. 86(7), 3895(1999) ; https://doi.org/10.1063/1.371306
[19] A. Moliton, "Electronique et Optoélectronique Organiques", Springer-Verlag, (2011); https://doi.org/10.1007/978-2-8178-0103-2
[20] K. Narayan, S. Varadharajaperumal, G.M. Rao, M.M. Varma, T. Srinivas, Current Applied Physics 13(1), 18(2013) ; https://doi.org/10.1016/j.cap.2012.06.004
[21] K. Peters, S. Raupp, H. Hummel, M. Bruns, P. Scharfer, W.Schabel, AIP Advances 6(6), 065108 (2016) ; https://doi.org/10.1063/1.4953845
[22] S.J. Zou, Yang Shen, F.M. Xie, J.D. Chen, Y.Q. Li, J.X. Tang, Mater. Chem. Front. 4, 788(2020) ; https://doi.org/10.1039/C9QM00716D
[23] J.H .Jou, J.W.Weng, S.D. Chavhan , R. A. K. Yadav, T.W. Liang, J. Phys. D: Appl. Phys. 51(45),454002 (2018) ; https://doi.org/10.1088/1361-6463/aad951
[24] T. Asadaa, S. Kosekia, Organic Electronics 53, 141, (2018) ; https://doi.org/10.1016/j.orgel.2017.11.025
[25] Shahnawaz, S. S. Swayamprabha, M. R. Nagar, R. A. Yadav, S. Gull, D. K. Dubey ,J. Jou, J. Mater. Chem. C, 7(24), 7144(2019) ; https://doi.org/10.1039/C9TC01712G
[26] N. Liu , S. Mei , D. Sun , W. Shi , J. Feng , Y. Zhou ,F. Mei, J. Xu, Y. Jiang, X. Cao, Micromachines, 10(5), 344(2019) ; https://doi.org/10.3390/mi10050344
[27] Y. S.Kim, J.H. Kim, J. S. Kim, K.T. No, J. Chem. Inf. Comput. Sci. 2002, 42(1), 75(2002).
[28] H. Wang, "Simulation of Organic Light Emitting Diode and Organic Photovoltaic Device", Thesis, University of Rochester New York, 2012 ; https://doi.org/10.1021/ci0103018
[28] H. Lee, Y. Hwang, T. Won, J. Korean Physical Society 66(1),100(2015) ; https://doi.org/10.3938/jkps.66.100
[29] R.A.K. Yadav, D.K. Dubey, S.Z. Chen, T.W. Liang, J.H. Jou, Scientific Reports 10(1), 9915(2020) ; https://doi.org/10.1038/s41598-020-66946-2
[30] A. Salehi, C.Dong, D.H. Shin, L. Zhu, C. Papa, A.T. Bui, F.N. Castellano, F. So, Nature Communications 10(1), 2305(2019) ; https://doi.org/10.1038/s41467-019-10260-7
[31] K. Kim, Y. Hwang, T. Won, Advanced Materials Research 629, 224(2012) ; https://doi.org/10.4028/www.scientific.net/AMR.629.224
[32] L. Zhang , L. Wang, W.J. Wu , M. Chan, IEEE Transactions on Electronic Devices 66(1), 139(2018) ; https://doi.org/10.1109/TED.2018.2843681
[33] C. Weichsel, L. Burtone, S. Reineke, I. Hintschich, M.C. Gather, K. Leo, B. Lüssem, Physical REV B 86(7) 075204(2012) ; https://doi.org/10.1103/PhysRevB.86.075204
[34] Y. Noguchi, Y. Miyazaki , Y. Tanaka , N. Sato , Y. Nakayama, T.D. Schmidt, W. Brütting, H. Ishii, J. Appl. Phys. 111(11), 114508(2012) ; https://doi.org/10.1063/1.4724349
[35] W.W. Zhang, Z.X. Wu, Y.W. Liu, J. Dong, X.W. Yan, X. Hou. Chinese Phys. Lett. 32(8), 087201(2015) ; https://doi.org/10.1088/0256-307X/32/8/087201

[36] M. Minagawa, Y. Tusuchida, K. Takahashi, A. Takahash, ITE Trans, on MTA. 3(2), 127(2015) ; https://doi.org/10.3169/mta.3.127

[37] J. Li, B. Qiao, S. Zhao, D. Song, C. Zhang, Z. Xu, Organic Electronics 83, 105756 (2020) ; https://doi.org/10.1016/j.orgel.2020.105756

[38] S. Züfle, S. Altazin, A. Hofmann, L. Jäger,, M. T. Neukom,W. Brütting, B. Ruhstaller, Journal of Applied Physics 122(11), 115502 (2017) ; https://doi.org/10.1063/1.4992041

[39] W. Sotoyama, T. Satoh, M. Kinoshita, M. Tobise, K.. Kawato, T. Ise, H. Takizawa, S. Yamashita, Fuji film research and development, No .55, (2010).

[40] M.K. Wei, C.W. Lin, C.C. Yang, Y.W. Kiang, J.H. Lee, H.Y. Lin, Int. J. Mol. Sci. 11(4), 1527 (2010) ; https://doi.org/10.3390/ijms11041527

[41] C.C. Lee, M.Y. Chang, P.T. Huang, Y.C. Chen, Y. Chang, J. Appl. Phys. 101(11), 114501(2007) ; https://doi.org/10.1063/1.2738445

[42] Y. Choe, S.Y. Park, D.W. Park, W. Kim, Macromolecular Research 14(1), 38(2006) ; https://doi.org/10.1007/BF03219066